Journal of Electronics and Electrical Engineering
https://ojs.wiserpub.com/index.php/JEEE/

Article

Dynamic Modeling and Chaos Suppression of the Permanent Magnet Synchronous Motor Drive with Sliding Mode Control

Mohammad Yousefzadeh[1,*], Hussein Eliasi[1] and Morteza Jalilirad[2]

[1]Faculty of Electrical and Computer Engineering, University of Birjand, Birjand, Iran
[2]Department of Electronics, Telecommunications and Informatics, University of Aveiro, Aveiro, Portugal
E-mail: mm.yousefzadeh68@gmail.com

Received: 3 August 2023; **Revised:** 1 September 2023; **Accepted:** 26 September 2023

Abstract: The permanent magnet synchronous motor (PMSM) is mathematically modeled and simulated in this study using MATLAB. PMSM is a nonlinear, multi-variable and time-varying system and due to nonlinearities and its strong coupling between its variables, the dynamical behaviour of the PMSM is complex. Therefore, under specified parameters and conditions, chaotic undesirable phenomenon arise in the PMSM. For a chaotic PMSM drive system, this paper proposes a sliding mode control (SMC) approach based on the Lyapunov stability theory to control and suppress the chaotic motion emergence. Firstly, the dynamic characteristics of the state equations of the PMSM drive system is analysed and demonstrated that it will appear chaos phenomenon at some certain parameters. Finally, the SMC strategy and Lyapunov stability theory are combined to introduce a sliding surface and produce a control rule. Simulation results are presented to verify that the proposed strategy can be successfully employed to control a chaotic PMSM and make the system asymptotically stable to the equilibrium point.

***Keywords*:** PMSM, dynamic modeling, chaotic systems, Lyapunov stability theory, SMC

1. Introduction

By using the permanent magnet (PM) to create a significant air gap in the magnetic flux, high-efficiency PM motors can be made. The PMSM is a type of very effective and powerful synchronous motor in which the rotor's PM produces the field excitation in the stator windings. The advantages of the PMSM's dependable functioning, straightforward design, and high-power density have led to its widespread acceptance for industry applications [1,2]. It finds widespread application in several fields, including robotics, wind turbines, electric vehicles, pumps, electric marine propulsion, motor drives, various servo systems, and home appliances [3–11].

Chaos is defined as long-term, non-periodic behaviour in a deterministic system that exhibits sensitive dependence to the initial conditions. Nonlinear dynamics underlie chaotic phenomenon in systems and foundational characteristics of chaotic behaviuor arise from its internal structure. The chaos theory is an interdisciplinary area of scientific study and is described as a branch of mathematics and computer science that studies the dynamic properties of nonlinear systems which are highly sensitive to the initial conditions. In order to investigate the chaotic behaviour of such systems, Lyapunov exponents and the compactness property of the phase space are two important measures that may be employed. Each chaotic attractor has an infinite number of unstable periodic orbits. consequently, chaotic motion emerges when the system states move in the neighborhood of one of these unstable periodic orbits for a short period and then fall close to another orbit for a limited time. This mechanism results in chaotic oscillation in which the system states move unpredictably for a long time. Chaotic systems are nonlinear and complex systems and prediction difficulty, broadband noise, and

DOI: https://doi.org/10.37256/jeee.2220233484

sensitivity to initial condition variations are counted as inherent characteristics in their response. The aim of chaos control is to stabilize the chaotic wandering of the system's states about its equilibrium points [12,13].

The importance of researching chaos in electric motors is due to how many different real-world scenarios it may be applied to right away. For instance, electric motors are crucial components of industrial equipment, electrical locomotives, and thruster drives in electrical submersibles [14]. In the late 1980s, [15] reported on the prevalence of chaos in motor driving systems. Following that, other scholars studied chaos, its management, and its synchronization in various motor drive systems. The brushless DC motor (BLDCM) [16,17], PMSM [18–22], stepper motor (SM) [23], induction motor (IM) [24,25], switching reluctance motor (SRM) drive, and synchronous reluctance motor (SynRM) [26–28] were all examined for chaos.

The PMSM's dynamic model is nonlinear, and it even experiences chaotic attractors and Hopf bifurcation. This makes it challenging to regulate the PMSM to obtain the ideal dynamic performance, despite the widespread use of electrical drive-based PMSMs in industrial applications. The PMSM's chaotic behaviour is undesirable because it may compromise the motor's stability and lead to the drive system collapsing [29]. Over recent years, the analysis and control of chaos in electric motors have become a significant research topic owing to its practical and theoretical importance. In order to further enhance the system's performance, chaos control, which aims to suppress PMSM's undesirable chaotic behaviour, has drawn increasing interest from both the academic and industrial communities. Recently, a variety of control techniques, including the Ott, feedback linearization, Grebogi and Yorke (OGY) method, adaptive control, and time delay feedback have been successful in controlling chaos in PMSM [30–33].

In [34] the finite-time control is suggested for chaos suppression in the PMSM. Based on Lyapunov stability and finite-time stability theory, the chaos suppression in PMSM was analyzed. An equivalent-input-disturbance (EID)-based control method is proposed in [35] for chaotic phenomenon suppression in speed control for PMSM drive. In [36] control of chaotic PMSM has been addressed by developing four simple classic controllers, which are mathematically designed by using Lyapunov theory principle in order to asymptotic global stability. Single feedback control (SFC)has been used for the problem of chaos control of the PMSM in [37]. As a matter of fact, the aim of this study was to solve the problem of set-point regulation of a PMSM via SFC. The proposed SFC scheme with a simple structure, has been theoretically and numerically confirmed to be less conservative than some existing results. The electronic implementation of chaos control using a state feedback controller in order to suppress chaotic behavior and synchronization of a PMSM is presented in [38]. Through the circuit implementation on OrCAD-PSpice software, the physical feasibility of the proposed two single and simple controllers as well as the chaos synchronization have been verified. The [39] suggests a backstepping fuzzy adaptive approach-based nonlinear control strategy to suppress chaos in a PMSM. In the controller design, the system disturbance and the parameter uncertainty are considered. The system stability is verified using the Lyapunov method. Furthermore, adaptive fuzzy dynamic surface (DSC), finite-time adaptive fuzzy dynamic DSC method and command filter-based adaptive control have been presented for chaotic PMSM in [40–42].

Since chaotic phenomena widely happen in the PMSM, it is significant to study the chaos phenomena and to devise a method of suppressing such phenomena. Among the methods, SMC has seen the most research and applications. SMC is a nonlinear control technique that has remarkable properties such as robustness, accuracy, easy tuning and implementation. SMC systems are designed to drive the system states onto a particular surface in the state space, named sliding surface. When the sliding surface is reached, SMC keeps the states on the close neighborhood of the sliding surface. Since system state variables always attract to the sliding surface, SMC enables to control nonlinear processes subject to external disturbance and heavy uncertainties in the model. In addition, cotrolling a *n*th order system turn into cotrolling a first order system.

SMC is a two-step controller design: sliding surface design and SMC law selection. The first step involves the design of a sliding surface so that design specifications are satisfied by means of the sliding motion. The second step is pertained to the selection of a control law that will make the switching surface attractive to the system states. An SMC system's dynamic performance is dictated by the switching surface that must be used in order to switch the control structure.

Motivated by the above discussion, the aim of this paper is dynamic modeling of a PMSM and to construct a sliding mode controller in order to suppress chaotic unpleasant phenomenon in the state variables (speed and currents) and stabilize the dynamically chaotic PMSM drive system. After defining a sable sliding surface, an appropriate SMC law is produced by satisfying the reachability condition.

2. Dynamic Model of the PMSM for Simulink Simulation

A two-pole PMSM concept is shown in Figure 1. It created the mathematical model of the PMSM using a two-phase motor in the quadrature(q) and direct(d) axes. This method is used for the reason that the stator only needs to have one set of two windings, which results in conceptual simplicity. The rotor is made exclusively of magnets, not windings. Either a flux linkage source or a current source is applied to the magnets. The flux connections of the stator's q and d-axis windings are obtained from the fundamentals.

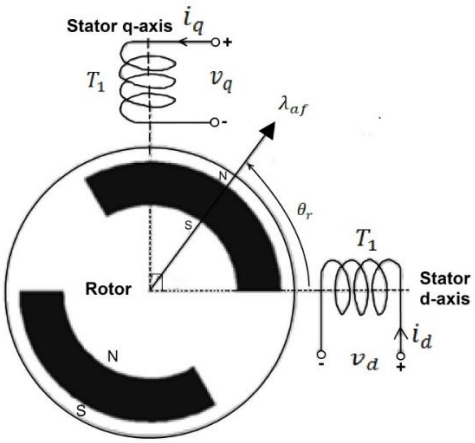

Figure 1. A two-pole PMSM structure.

The stator q and d-axis winding are displaced from one another by 90 electrical degrees in space, and the rotor flux linkage(magnetic) axis is at θ_r angle from the stator d-axis winding. When the q-axis pushes the d-axis in the opposite direction, it is assumed that the rotor rotates anticlockwise. The stator q and d-axes voltages are produced by adding the resistive voltage drop to the derivative of the flux in the q and d-axes windings.

$$\begin{aligned} V_{qs} &= R_q i_{qs} + \frac{d}{dt}\lambda_{qs} \\ V_{ds} &= R_d i_{ds} + \frac{d}{dt}\lambda_{ds} \end{aligned} \tag{1}$$

where V_{qs} and V_{ds} are the q and d-axes windings voltages respectively. The stator q and d-axes currents are known as i_{qs} and i_{ds}. The stator's q and d-axes resistances are R_q and R_d, λ_{qs} and λ_{ds} are q and d-axes flux linkages.

The stator q and d winding flux linkages Y_{qs} and Y_{ds} can be thought of as as the sum of the flux linkages resulting from their own excitation and the mutual flux linkages arising from other winding and are expressed in writing as:

$$\begin{aligned} Y_{qs} &= L_{qq} i_{qs} + L_{qd} i_{ds} + \lambda_{as} \sin\theta_r \\ Y_{ds} &= L_{dd} i_{qs} + L_{qd} i_{ds} + \lambda_{as} \cos\theta_r \end{aligned} \tag{2}$$

where the instantaneous position of the rotor is denoted by θ_r. λ_{af} is the flux linkage due to the rotor's permanent magnet linking the stator. The resistances, $R_s = R_q = R_d$, are equal since the windings are balanced.

The stator q and d-axes stator voltages can therefore be written as using the resistive voltage drops and flux connections.

$$\begin{aligned} V_{qs} &= R_s i_{qs} + i_{qs}\frac{d}{dt}L_{qq} + L_{qq}\frac{d}{dt}i_{qs} + i_{ds}\frac{d}{dt}L_{qd} + \lambda_{af}\frac{d}{dt}\sin\theta_r \\ V_{ds} &= R_s i_{ds} + i_{qs}\frac{d}{dt}L_{qd} + L_{qd}\frac{d}{dt}i_{qs} + i_{ds}\frac{d}{dt}L_{dd} + \lambda_{af}\frac{d}{dt}\cos\theta_r \end{aligned} \tag{3}$$

L_{qq} and L_{dd} are, respectively, the self-inductances of the q and d-axes windings. The reciprocal inductances between two windings are L_{qd} and L_{dq}. L_{qd} and L_{dq} are equivalent thanks to the symmetry of the q and d-axes windings. L_1 and L_2 are the stator self-inductance and mutual inductance respectively. There are many terms that rely on the rotor position when the self and mutual inductances are substituted into the stator voltage equations. On the other hand, with surface-mounted PMSM, the inductances are identical, and L_2 is thus equal to zero. The

position-dependent terms also vanish in the second term of the matrix, leading to a straightforward expression for surface-mounted PMSM in the stator reference frame. After that, it is provided by

$$\begin{bmatrix} V_{qs} \\ V_{ds} \end{bmatrix} = R_s \begin{bmatrix} i_{qs} \\ i_{ds} \end{bmatrix} + \begin{bmatrix} L_1 & 0 \\ 0 & L_2 \end{bmatrix} \frac{d}{dt} \begin{bmatrix} i_{qs} \\ i_{ds} \end{bmatrix} + \lambda_{af} \theta_r \begin{bmatrix} \cos\theta_r \\ -\sin\theta_r \end{bmatrix} \tag{4}$$

The q and d-axes inductances of salient pole PMSMs depend on the position of the rotor. By eliminating the rotor position dependency of the inductances using a transformation matrix, the relationship between currents and flux linkages is determined by the matrix including the rotor position-related terms in a unique manner.

A distinct perspective on the system is provided by reference frames, which also dramatically simplify the system equations. The wound rotor's and the PMSMs' dynamic system equations are affected by the position of the independent rotor field, which also influences the induced emf. Viewing the entire system from the perspective of the rotor, leads to the simplification and compactness of the system equations, and the inductance matrix (equation 4) becomes independent of the rotor position. The transformation matrix's definition of the correlation between the variables in the rotor reference frame *dr* – *qr* and the stationary reference frame *d* – *q* is as follows:

$$\begin{bmatrix} f_q \\ f_d \end{bmatrix} = \begin{bmatrix} \cos\theta_r & \sin\theta_r \\ -\sin\theta_r & \cos\theta_r \end{bmatrix} \begin{bmatrix} f_q^r \\ f_d^r \end{bmatrix} \tag{5}$$

where *f* is considered as voltage, current, or flux linkages variable. The stator voltage (V_{qs}, V_{ds}), electromagnetic torque (T_e), and motor angular velocity (ω_m) equations that make up the PMSM model in the rotor reference frame are generated as:

$$\begin{bmatrix} V_{qs} \\ V_{ds} \end{bmatrix} = \begin{bmatrix} R_s + \frac{d}{dt}L_q & \omega_r L_d \\ -\omega_r L_d & R_s + \frac{d}{dt}L_d \end{bmatrix} \begin{bmatrix} i_{qs} \\ i_{ds} \end{bmatrix} + \begin{bmatrix} \omega_r \lambda_{af} \\ 0 \end{bmatrix} \tag{6}$$

$$T_e = \left(\frac{3}{2}\right)\left(\frac{P}{2}\right)\left[\lambda_{af} + \left(L_d - L_d\right) i_{dr}^r\right] i_{qr}^r \tag{7}$$

$$J \frac{d\omega_m}{d_t} = T_e - T_l - B\omega_m \tag{8}$$

where ω_m and ω_r represent the rotor mechanical speed (motor angular velocity) and rotor electrical speed respectively. *J* considers the sum of the shaft and load inertia. T_l is load torque, *B* and *P* are the friction coefficient and number of stator poles respectively.

3. Dynamic Model of the Chaotic PMSM Drive System

The dimensionless dynamic model of a PMSM with a smooth air gap [30] can be described in the following ways:

$$\begin{aligned} \frac{di_{ds}}{dt} &= -i_{ds} + \omega_m i_{qs} + \bar{v}_{ds} \\ \frac{di_{qs}}{dt} &= -i_{qs} - \omega_m i_{ds} + \gamma\omega_m + \bar{v}_{qs} \\ \frac{d\omega_m}{dt} &= \sigma\left(i_{qs} - \omega_m\right) - \bar{T}_l \end{aligned} \tag{9}$$

where i_{qs}, i_{ds} and ω_m are state variables, in which i_{ds}, i_{qs} denote the *d* – *q* axis stator currents and ω_m is motor angular speed. $\sigma > 0$ and $\gamma > 0$ are system operating parameters. $\bar{v}_{ds}$ and $\bar{v}_{qs}$ denote *d* – *q* axis voltages and $\bar{T}_l$ represents the external load torque. operating parameters formulation of the σ and γ can be presented as following:

$$\gamma = -\frac{\varphi_r}{kL_q}, \quad k = -\frac{B}{n_p \tau \varphi_r}$$

$$\sigma = \frac{B\tau}{J}, \quad \tau = \frac{L_q}{R_s}$$

where φ_r, n_p and τ are the permanent magnet flux, number of pol-pairs and time constant of the stator winding respectively.

This study only considers the case that the system is unforced. This case can be considered as that, after a system operating period, the external inputs are set to zero. Namely, if we select $\bar{T}_l = \bar{v}_{ds} = \bar{v}_{qs} = 0$, after that system (9) becomes an unforced system as:

$$\begin{aligned} \frac{di_{ds}}{dt} &= -i_{ds} + \omega_m i_{qs} \\ \frac{di_{qs}}{dt} &= -i_{qs} - \omega_m i_{ds} + \gamma\omega_m \\ \frac{d\omega_m}{dt} &= \sigma\left(i_{qs} - \omega_m\right) \end{aligned} \tag{10}$$

The chaos phenomenon and bifurcation of the system (10) have been studied in several past researches. For more details on the chaotic phenomena analysis and bifurcation criterion of the PMSM and operating parameters formulation, we can refer to [43]. When the initial conditions of system states and the operating parameters γ and σ fall in a certain range of values, it has been found that the PMSM experiences chaotic behaviour. For example, for γ = 20 and σ = 5.45, the PMSM displays chaos [34,43]. Figure 2 illustrates a typical chaotic attractor. The stabilization of the PMSM drive system can be disrupted by these chaotic oscillations.

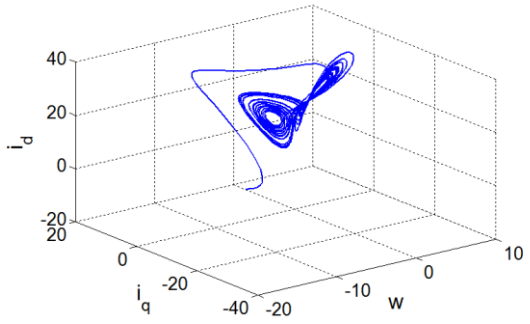

Figure 2. The chaotic attractor of PMSM with operating parameters γ = 20 and σ = 5.45.

4. Sliding Mode Controller Design

The PMSM drive system's performance may suffer as a result of the chaotic oscillations. In order to control chaos in the PMSM drive, $u(t)$ is used as a movable variable. We provide the following notations for convenience of use:

$$\begin{cases} x = \omega_m \\ y = i_{qs} \\ z = i_{ds} \end{cases} \tag{11}$$

Following that, the dynamic model of the PMSM drive described in (10) can be expressed as:

$$\begin{cases} \frac{dx}{dt} = \sigma\left(y - x\right) + U \\ \frac{dy}{dt} = -y - xz + \gamma x \\ \frac{dz}{dt} = -z + xy \end{cases} \tag{12}$$

The aim of control in this study is to design an SMC with the state variables convergent to the origin.

A sliding mode controller is created in two steps. After defining a stable sliding surface, a suitable control rule is selected to trend the state variables towards the sliding surface. The following definition of an adaptable sliding surface is based on [44]:

$$s(t) = x(t) + f(t) \tag{13}$$

where $s(t) \in R$ and $f(t)$ is an adaptive function satisfy

$$\frac{df}{dt} = rx - \gamma xy \tag{14}$$

where $r > 0$ is the design parameter. The following equations must be true for the system to function in sliding mode:

$$s(t) = x(t) + f(t) = 0 \tag{15}$$

$$\frac{s(t)}{dt} = \frac{x(t)}{dt} + \frac{f(t)}{dt} = 0 \tag{16}$$

Then we have

$$\frac{x(t)}{dt} = -\frac{f(t)}{dt} = -rx + \gamma xy \tag{17}$$

Therefore for Equation (16), the dynamics of sliding mode can be rewritten as:

$$\begin{cases} \dfrac{dx}{dt} = -rx + \gamma xy \\ \dfrac{dy}{dt} = -y - xz + \gamma x + \bar{v}_{qs} \\ \dfrac{dz}{dt} = -z + xy + \bar{v}_{ds} \end{cases} \tag{18}$$

Now, the stability of the closed-loop system can be investigated using the Lyapunov stability theory. Examining the next potential option for the Lyapunov function.

$$V(t) = \frac{1}{2}\left(x^2 + y^2 + z^2\right) > 0 \tag{19}$$

The time derivative of $V(t)$ is given by:

$$\begin{aligned} \dot{V}(t) &= x\dot{x} + y\dot{y} + z\dot{z} = x(-rx + \gamma xy) + y(-y - zx + \gamma x) + z(-z + yx) \\ &= -rx^2 - y^2 - z^2 \end{aligned} \tag{20}$$

where $\dot{V}(t) \le 0$. Based on Lyapunov stability theory, the sliding mode motion on the sliding mode manifold is stable and ensures:

$$\lim_{t \to \infty} \|x, y, z\| = 0 \tag{21}$$

When the correct switching manifold has been established, the next step is to develop a SMC mechanism to guide the trajectories of the system onto the sliding surface $s = 0$. Since the closed-loop system places in a sliding phase, we are aware that $\dot{s} = 0$. Then we will have:

$$u(t) = -\sigma(y - x) - rx + \gamma xy - ksign(s) \tag{22}$$

In (22), $k > 0$ and is considered as a design parameter. According to the above discussions, we can get the following results:

Theorem 1: For the chaotic PMSM system (12), the system's state variables converge to the sliding surface $s = 0$ if the sliding mode surface is chosen as (13) and the control input is configured as (22).

Proof 1: Define the following Lyapunov function:

$$V = \frac{1}{2}s^2 \tag{23}$$

Its time derivative is given and from (4–6), we have:

$$\dot{V} = s\dot{s} = s(\dot{x} + \dot{f}) \tag{24}$$

By using (4), (6), and (14) we can get

$$\dot{V} = k|s| \tag{25}$$

The reaching requirement is always satisfied, as we can infer. This concludes the evidence.

5. Simulation Results

Figures 3–6 show different sub-models and the complete simulink model of the PMSM in accordance with equations (6), (7), and (8). Figure 7 displays the motor's dynamic responses when combined with Table 1's parameters. The simulation results of dynamic responses including motor speed and electromagnetic torque, motor current and rotor position given in Figure 7, verify the validity of the proposed simulink scheme.

Table1. PMSM parameters used in simulation

Parameter	V_{rms} (V)	P	R_s (Ω)	L_d (H)	L_q (H)	flux (Wb)	B (kg/m^2)	J (N/ms)
Value	220	4	1.2	0.0078	0.0078	0.1540	$4.6752e^{-5}$	$2.0095e^{-5}$

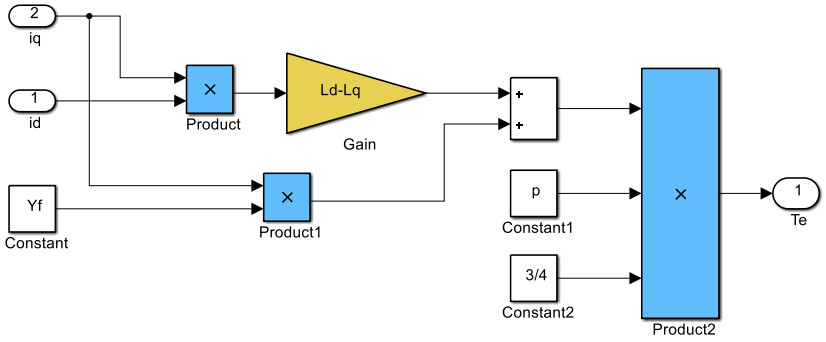

Figure 3. Electromagnetic torque sub-model

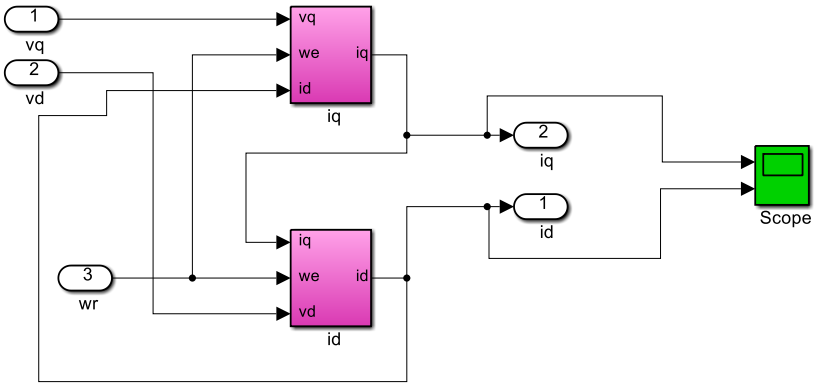

Figure 4. Current equations sub-model

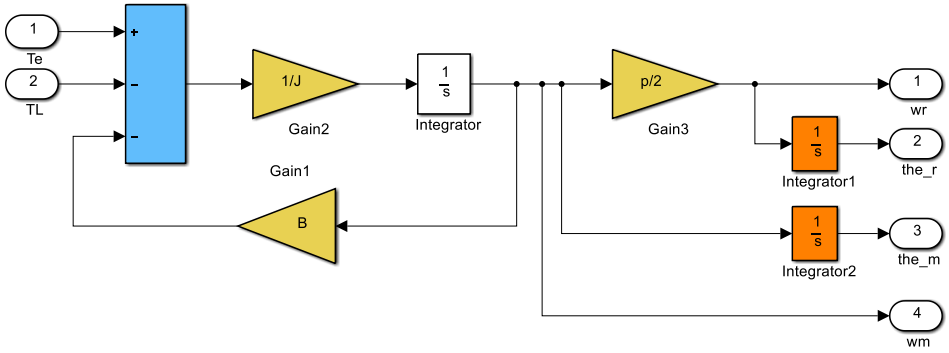

Figure 5. Motor speed and rotor position sub-model

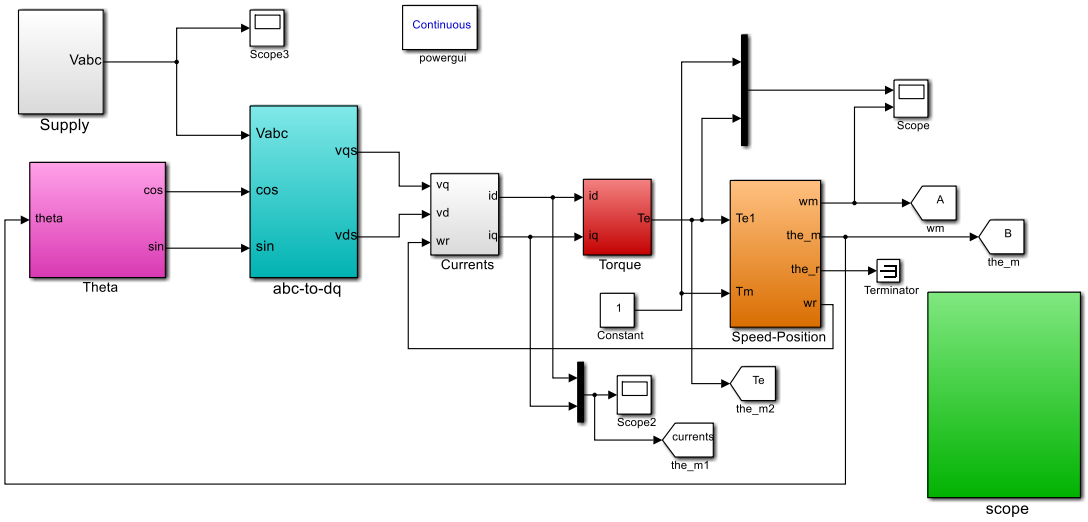

Figure 6. Complete simulink model of the PMSM

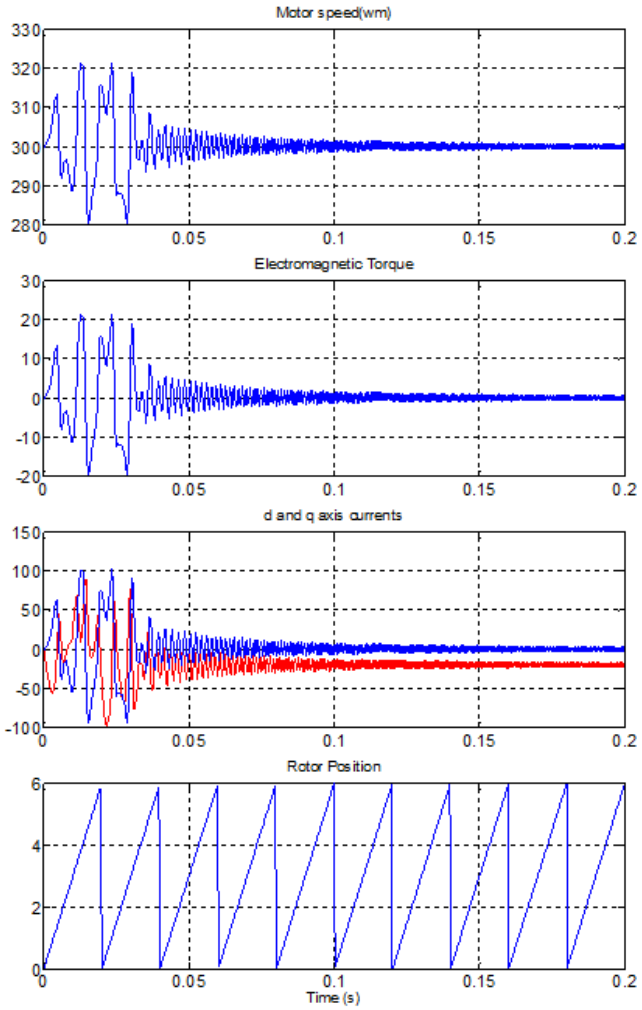

Figure 7. Dynamic responses of the PMSM

To demonstrate the efficacy of the suggested control strategy, this paper provides an example. The simulation results are compared to the finite-time control proposed in [34]. Initial values $[x, y, z] = [-5, 10, -1]^T$. The selection of $r = k = 2$ as the design parameters. The chosen system parameters are $\gamma = 20$ and $\sigma = 5.45$. Figure 8 displays the state variables reactions of the chaotic PMSM if $u(t) = 0$.

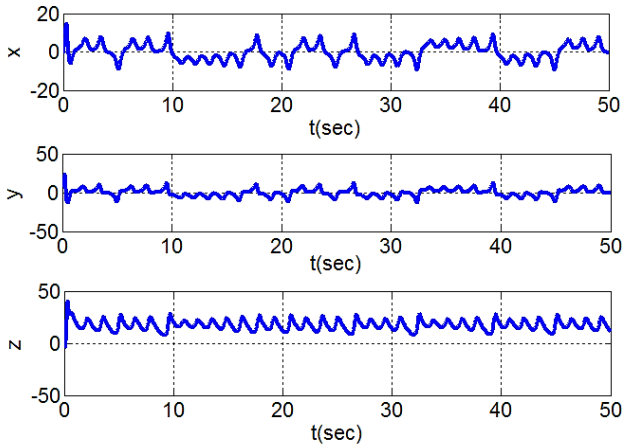

Figure 8. State variables of the PMSM drive system without control

Figures 9–13 display the simulation results if the control input as (22) is employed. The sliding surface curve and control signal obtained from the proposed approach are shown in Figures 9 and 10. Figures 11, 12 and 13 illustrate the system state variables for various controllers.

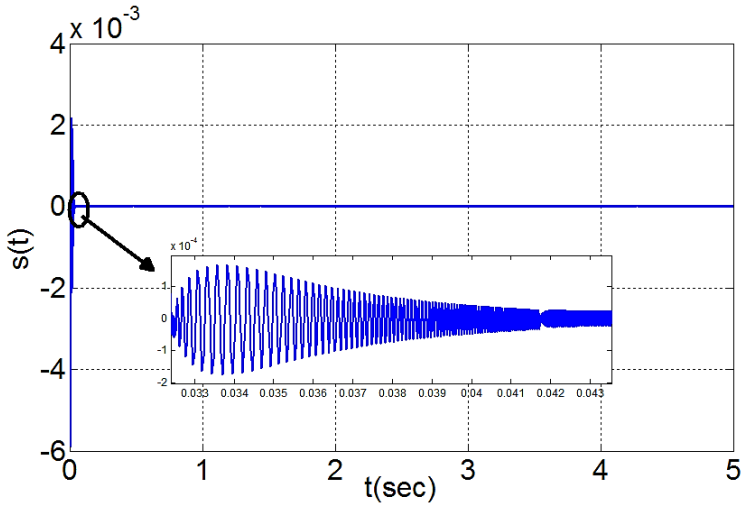

Figure 9. The sliding surface

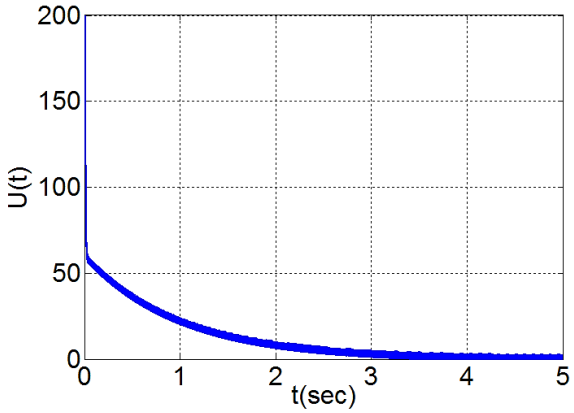

Figure 10. The control input

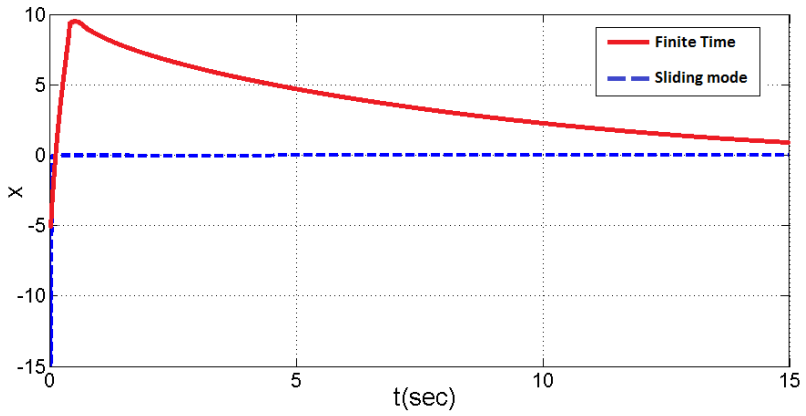

Figure 11. The response of state variable x of the controlled PMSM under different controller

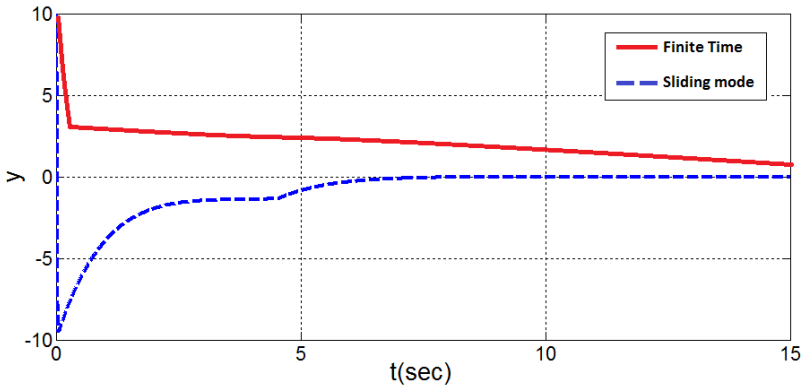

Figure 12. The response of state variable y of the controlled PMSM under different controller

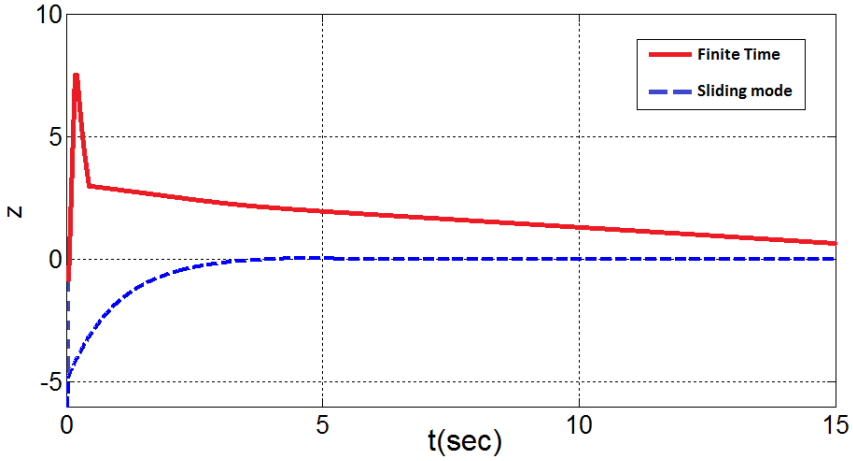

Figure 13. The response of state variable z of the controlled PMSM under different controller

The results of the simulation demonstrate that the suggested approach is effective in regulating the chaotic PMSM system, and the tracking performance is good. As seen from Figures 11, 12 and 13, the system state variables including x = ω_m, y = i_{qs}, and z = i_{ds} converge to the sliding surface exponentially. The process of the reaching system to the sliding surface from any initial state is called reaching mode. According to the designed trajectory, the reaching law is able to make the system states reach the sliding surface and improve the dynamic behaviour of the reaching mode.

Also, the comparative analysis of the system states from Figures 11–13 confirms that the designed SMC controller can achieve chaos suppression in the PMSM drive system with fewer overshoots and oscillations. Moreover, the proposed control has stabilized the system faster than the finite-time control proposed in [34].

6. Conclusion

The dynamic simulation-based PMSM model is implemented in MATLAB in this article. The simulation's findings reflect the PMSM's performance traits. In the graph, the motor's speed, stator currents, electromagnetic torque, and rotor position are all displayed at the same time. A SMC strategy has been presented to build a controller for a chaotic PMSM drive. For determining the stability in sliding phase motion, a switching manifold is defined. Lyanpunov-based stability analysis and the simulation results in MATLAB software serve as evidence of this method's effectiveness due to its capacity to successfully eliminate chattering in sliding mode control and suppress chaotic phenomena in the PMSM drive system. Moreover, the comparative simulation shows better performance of the proposed SMC than finite-time method.

Conflict of Interest

There is no conflict of interest for this study.

References

[1] Bak, Y.; Lee, K.-B. Constant Speed Control of a Permanent-Magnet Synchronous Motor Using a Reverse Matrix Converter Under Variable Generator Input Conditions. *IEEE J. Emerg. Sel. Top. Power Electron.* **2017**, *6*, 315–326, https://doi.org/10.1109/jestpe.2017.2715046.

[2] Lu, S.; Wang, X.; Li, Y. Adaptive neural network control for fractional-order PMSM with time delay based on command filtered backstepping. *AIP Adv.* **2019**, *9*, 055105, https://doi.org/10.1063/1.5094574.

[3] Chen, B.; Liu, X.; Liu, K.; Lin, C. Adaptive fuzzy tracking control of nonlinear MIMO systems with time-varying delays. *Fuzzy Sets Syst.* **2012**, *217*, 1–21, https://doi.org/10.1016/j.fss.2012.11.002.

[4] Qi, L.; Shi, H. Adaptive position tracking control of permanent magnet synchronous motor based on RBF f ast terminal sliding mode control. *Neurocomputing* **2013**, *115*, 23–30, https://doi.org/10.1016/j.neucom.201 2.11.018.

[5] Cuenot, J.; Zaim, S.; Nahid-Mobarakeh, B.; Pierfederici, S.; Monmasson, E.; Meuret, R.; Meibody-Tabar, F. Overall Size Optimization of a High-Speed Starter Using a Quasi-Z-Source Inverter. *IEEE Trans. Transp. Electrification* **2017**, *3*, 891–900, https://doi.org/10.1109/tte.2017.2738022.

[6] Hong, D.-K.; Hwang, W.; Lee, J.-Y.; Woo, B.-C. Design, Analysis, and Experimental Validation of a Permanent Magnet Synchronous Motor for Articulated Robot Applications. *IEEE Trans. Magn.* **2017**, *54*, 1–4, https://doi.org/10.1109/tmag.2017.2752080.

[7] Wu, Y.-J.; Li, G.-F. Adaptive disturbance compensation finite control set optimal control for PMSM systems based on sliding mode extended state observer. *Mech. Syst. Signal Process.* **2018**, *98*, 402–414, https://doi.org/10.1016/j.ymssp.2017.05.007.

[8] Zhang, X.-Y.; Lin, Y. A Robust Adaptive Dynamic Surface Control for Nonlinear Systems with Hysteresis Input. *Acta Autom. Sin.* **2010**, *36*, 1264–1271, https://doi.org/10.1016/s1874-1029(09)60053-7.

[9] Mao, W.-L.; Liu, G.-Y. Development of an Adaptive Fuzzy Sliding Mode Trajectory Control Strategy for T wo-axis PMSM-Driven Stage Application. *Int. J. Fuzzy Syst.* **2019**, *21*, 793–808, https://doi.org/10.1007/s4 0815-018-0596-y.

[10] Kommuri, S.K.; Defoort, M.; Karimi, H.R.; Veluvolu, K.C. A Robust Observer-Based Sensor Fault-Toleran t Control for PMSM in Electric Vehicles. *IEEE Trans. Ind. Electron.* **2016**, *63*, 7671–7681, https://doi.org/1 0.1109/tie.2016.2590993.

[11] Sun, Y.; Chen, L.; Ma, G.; Li, C. Adaptive neural network tracking control for multiple uncertain Euler–La grange systems with communication delays. *J. Frankl. Inst.* **2017**, *354*, 2677–2698, https://doi.org/10.1016/ j.jfranklin.2017.01.021.

[12] Encyclopedia Britannica. Chaos theory. Available online: https://www.britannica.com/science/chaos-theory (Accessed on 26 August 2023).

[13] Schimmack, M.; Mercorelli, P. Anatomy of Chua's System - Nonlinear Dynamic Electronics for Chaos in the Lab. *IFAC-PapersOnLine* **2022**, *55*, 302–307, https://doi.org/10.1016/j.ifacol.2022.09.296.

[14] Chau, K. T.; Wang, Z. Chaos in Electric Drive Systems: Analysis, Control and Application. Wiley-IEEE Pr ess: NJ, USA, 2011.

[15] Kuroe, Y.; Hayashi, S. Analysis of bifurcation in power electronic induction motor drive systems. **2003**, https://doi.org/10.1109/pesc.1989.48578.
[16] Hemati, N. Strange attractors in brushless DC motors. *IEEE Trans. Circuits Syst. I: Regul. Pap.* **1994**, *41*, 40–45, https://doi.org/10.1109/81.260218.
[17] Liu, D.; Zhou, G.; Liao, X. Global exponential stabilization for chaotic brushless DC motor with simpler controllers. *Trans. Inst. Meas. Control.* **2019**, *41*, 2678–2684, https://doi.org/10.1177/0142331218802355.
[18] Li, Z.; Zhang, B.; Tian, L.; Mao, Z.; Pong, M. Strange attractors in permanent-magnet synchronous motors. **1999**, https://doi.org/10.1109/peds.1999.794552.
[19] Zribi, M.; Oteafy, A.; Smaoui, N. Controlling chaos in the permanent magnet synchronous motor. *Chaos, Solitons Fractals* **2009**, *41*, 1266–1276, https://doi.org/10.1016/j.chaos.2008.05.019.
[20] Ye, J.; Yang, J.; Xie, D.; Huang, B.; Cai, H. Strong Robust and Optimal Chaos Control for Permanent Mag net Linear Synchronous Motor. *IEEE Access* **2019**, *7*, 57907–57916, https://doi.org/10.1109/access.2019.29 13900.
[21] Zwerger, T.; Mercorelli, P. Combining SMC and MTPA Using an EKF to Estimate Parameters and States of an Interior PMSM. **2019**, 1–6, https://doi.org/10.1109/carpathiancc.2019.8766063.
[22] Zwerger, T.; Mercorelli, P. Combining an Internal SMC with an External MTPA Control Loop for an Interior PMSM. **2018**, 674–679, https://doi.org/10.1109/mmar.2018.8485900.
[23] Pera, M. C.; Robert, B.; Goeldel, C. Quasiperiodicity and chaos in a step motor. In Proceedings of the 8th European Conference on Power Electronics and Applications, Lausanne, Switzerland, 7-9 September 1999.
[24] Zhang, B.; Lu, Y.; Mao, Z. Bifurcations and chaos in indirect field-oriented control of induction motors. *J. Control Theory Appl.* **2004**, *2*, 353–357, https://doi.org/10.1007/s11768-004-0039-1.
[25] Messadi, M.; Mellit, A. Control of chaos in an induction motor system with LMI predictive control and exp erimental circuit validation. *Chaos, Solitons Fractals* **2017**, *97*, 51–58, https://doi.org/10.1016/j.chaos.2017. 02.005.
[26] Chen, J.H.; Chau, K.T.; Chan, C.C.; Jiang, Q. Subharmonics and Chaos in Switched Reluctance Motor Drives. *IEEE Power Eng. Rev.* **2002**, *22*, 57–57, https://doi.org/10.1109/mper.2002.4311981.
[27] Gao, Y.; Chau, K. Hopf Bifurcation and Chaos in Synchronous Reluctance Motor Drives. *IEEE Trans. Energy Convers.* **2004**, *19*, 296–302, https://doi.org/10.1109/tec.2004.827012.
[28] Rajagopal, K.; Nazarimehr, F.; Karthikeyan, A.; Srinivasan, A.; Jafari, S. Fractional Order Synchronous Reluctance Motor: Analysis, Chaos Control and FPGA Implementation. *Asian J. Control.* **2017**, *20*, 1979–1993, https://doi.org/10.1002/asjc.1690.
[29] Wang, L.; Fan, J.; Wang, Z.; Zhan, B.; Li, J. Dynamic Analysis and Control of a Permanent Magnet Synchronous Motor with External Perturbation. *J. Dyn. Syst. Meas. Control.* **2015**, *138*, 011003, https://doi.org/10.1115/1.4031726.
[30] Yu, J.; Chen, B.; Yu, H.; Gao, J. Adaptive fuzzy tracking control for the chaotic permanent magnet synchronous motor drive system via backstepping. *Nonlinear Anal. Real World Appl.* **2011**, *12*, 671–681, https://doi.org/10.1016/j.nonrwa.2010.07.009.
[31] Yu, J.; Shi, P.; Liu, J. Intelligent Backstepping Control for the Alternating-Current Drive Systems. **2021**, htt ps://doi.org/10.1007/978-3-030-67723-7.
[32] Ren, H.; Liu, D. Nonlinear feedback control of chaos in permanent magnet synchronous motor. *IEEE Trans. Circuits Syst. II: Analog. Digit. Signal Process.* **2006**, *53*, 45–50, https://doi.org/10.1109/tcsii.2005.854592.
[33] Lu, S.; Wang, X.; Wang, L. Finite-time adaptive neural network control for fractional-order chaotic PMSM via command filtered backstepping. *Adv. Differ. Equations* **2020**, *2020*, 1–21, https://doi.org/10.1186/s1366 2-020-02572-6.
[34] Hou, Y.-Y. Finite-Time Chaos Suppression of Permanent Magnet Synchronous Motor Systems. *Entropy* **2014**, *16*, 2234–2243, https://doi.org/10.3390/e16042234.
[35] Yin, X.; She, J.; Liu, Z.; Wu, M.; Kaynak, O. Chaos suppression in speed control for permanent-magnet-sy nchronous-motor drive system. *J. Frankl. Inst.* **2020**, *357*, 13283–13303, https://doi.org/10.1016/j.jfranklin. 2020.05.007.
[36] Iqbal, A.; Singh, G.K. Chaos control of permanent magnet synchronous motor using simple controllers. *Trans. Inst. Meas. Control.* **2018**, *41*, 2352–2364, https://doi.org/10.1177/0142331218799830.
[37] Hamidzadeh, S.M.; Yaghoobi, M. Chaos control of permanent magnet synchronous motors using single fee dback control. **2015**, 325–329, https://doi.org/10.1109/kbei.2015.7436066.

[38] Cheukem, A.; Tsafack, A.S.K.; Kingni, S.T.; André, C.C.; Pone, J.R.M. Permanent magnet synchronous motor: chaos control using single controller, synchronization and circuit implementation. *SN Appl. Sci.* **2020**, *2*, 1–11, https://doi.org/10.1007/s42452-020-2204-7.

[39] Zhang, J.; Sun, J.; Gu, H.; Poloei, H.; Karami, A. Control of PMSM chaos using backstepping-based adaptive fuzzy method in the presence of uncertainty and disturbance. *Syst. Sci. Control. Eng.* **2021**, *9*, 673–688, https://doi.org/10.1080/21642583.2021.1980130.

[40] Luo, S. Adaptive fuzzy dynamic surface control for the chaotic permanent magnet synchronous motor using Nussbaum gain. *Chaos: Interdiscip. J. Nonlinear Sci.* **2014**, *24*, 033135, https://doi.org/10.1063/1.4895810.

[41] Song, S.; Yu, J.; Zhao, L.; Cui, G. Finite-time fuzzy dynamic surface control for permanent magnet synchronous motor stochastic systems with input constraint and load disturbance. *Trans. Inst. Meas. Control.* **2022**, *44*, 1853–1861, https://doi.org/10.1177/01423312211065585.

[42] Zirkohi, M.M. Command filtering-based adaptive control for chaotic permanent magnet synchronous motor s considering practical considerations. *ISA Trans.* **2020**, *114*, 120–135, https://doi.org/10.1016/j.isatra.2020.12.036.

[43] Li, Z.; Park, J.B.; Joo, Y.H.; Zhang, B.; Chen, G. Bifurcations and chaos in a permanent-magnet synchrono us motor. *IEEE Trans. Circuits Syst. I: Regul. Pap.* **2002**, *49*, 383–387, https://doi.org/10.1109/81.989176.

[44] Dadras, S.; Momeni, H.R.; Majd, V.J. Sliding mode control for uncertain new chaotic dynamical system. *Chaos, Solitons Fractals* **2009**, *41*, 1857–1862, https://doi.org/10.1016/j.chaos.2008.07.054.